Article

Photochemical Grafting of *n*-Alkenes onto Carbon Surfaces: the Role of Photoelectron Ejection

Paula E. Colavita, Bin Sun, Kiu-Yuen Tse, and Robert J. Hamers

J. Am. Chem. Soc., **2007**, 129 (44), 13554-13565• DOI: 10.1021/ja073944y • Publication Date (Web): 10 October 2007

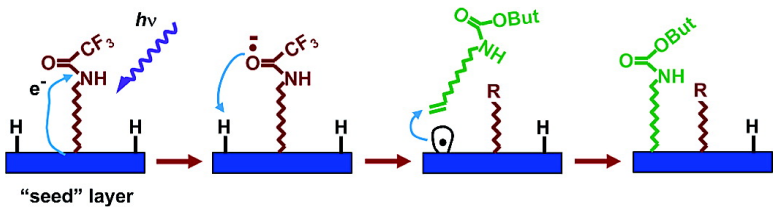

More About This Article

Additional resources and features associated with this article are available within the HTML version:

- Supporting Information
- Links to the 5 articles that cite this article, as of the time of this article download
- Access to high resolution figures
- Links to articles and content related to this article
- Copyright permission to reproduce figures and/or text from this article

View the Full Text HTML

J|A|C|S
ARTICLES
Published on Web 10/10/2007

Photochemical Grafting of *n*-Alkenes onto Carbon Surfaces: the Role of Photoelectron Ejection

Paula E. Colavita, Bin Sun, Kiu-Yuen Tse, and Robert J. Hamers*

Contribution from the Department of Chemistry, 1101 University Avenue, University of Wisconsin, Madison, Wisconsin 53706-1396

Received May 31, 2007; E-mail: rjhamers@facstaff.wisc.edu

Abstract: The grafting of molecular layers to carbon-based materials provides a way to combine the high chemical and thermal stability of these materials with surface properties such as chemical recognition or reactivity. The functionalization of surfaces with ultraviolet light has emerged as a way to modify difficult-to-functionalize materials, such as diamond. We have performed a combined experimental and computational investigation of the photochemical reaction of terminal alkenes with hydrogen-terminated carbon surfaces. 1-Alkenes carrying various terminal functional groups ($-NHCOCF_3$, $-NHCOO$(*tert*-butyl), $-COOCH_3$, $-CH_3$) were grafted from the neat liquids using 254 nm light. These layers were characterized using X-ray Photoelectron Spectroscopy and Infrared Reflectance Absorption Spectroscopy. Pronounced differences in reactivity were observed between the molecules: trifluoroacetamide-terminated alkenes grafted the fastest and yielded self-terminating layers after ~4 h. Ultraviolet photoelectron spectroscopy and photocurrent measurements show that the grafting reaction involves photoemission of electrons into the liquid. Density functional calculations show that the reactivites of the four molecules are correlated with their electron affinities, with the trifluoroacetamide group acting as the best electron acceptor and having the highest reactivity. Our results demonstrate that photoejection of electrons from the solid into the acceptor levels of the alkenes initiates the functionalization reaction and controls the overall rate. Finally, marginally reactive *n*-alkenes were induced to react and form dense monolayers by seeding the carbon surface with small amounts of a good electron acceptor, such as the trifluoroacetamide moiety. This study provides important new mechanistic insights into the use of ultraviolet light to initiate grafting of alkenes onto surfaces.

1. Introduction

The photochemical grafting of terminal alkenes under ultraviolet (UV) illumination is an important functionalization strategy widely used in the literature to chemically modify semiconductor surfaces, such as silicon,[1,2] germanium,[3] gallium nitride,[4] and diamond,[5,6] as well as other materials such as carbon nanofibers and glassy carbon.[7] While UV light can induce many surfaces to react with alkenes, many mechanistic aspects of the functionalization reactions remain poorly understood, and it is not clear whether different materials react via different mechanistic pathways. The grafting of alkenes to carbon-based materials is important because the C−C bonds formed at the interface confer the resulting monolayers with very high stability under a wide range of conditions.[8,9] Recent studies have shown that organic alkenes can be induced to react with diamond,[5,6,10] carbon nanofibers,[7] and amorphous carbon[8] and that the functionalized surfaces have excellent stability that make them attractive materials for applications in biosensing, bioimplants, or electrocatalysis.

Previous mechanistic studies on the photochemical functionalization of carbon in the form of diamond have shown that the functionalization reaction is initiated by the emission of a photoelectron into the liquid phase.[6,11] In diamond, electron ejection is facilitated by diamond's unusual property of negative electron affinity, in which the vacuum level lies below the conduction band edge.[12−16] In negative electron affinity materials, photoexcitation of electrons to the conduction band can yield barrier-free ejection of electrons.[12−16] Yet, the possible role of

(1) Cicero, R. L.; Linford, M. R.; Chidsey, C. E. D. *Langmuir* **2000**, *16*, 5688−5695.
(2) Linford, M. R.; Fenter, P.; Eisenberger, P. M.; Chidsey, C. E. D. *J. Am. Chem. Soc.* **1995**, *117*, 3145−3155.
(3) Choi, K.; Buriak, J. M. *Langmuir* **2000**, *16*, 7737−7741.
(4) Kim, H.; Colavita, P. E.; M., M. K.; Nichols, B. M.; Sun, B.; Uhlrich, J.; Wang, X. Y.; Kuech, T. F.; Hamers, R. J. *Langmuir* **2006**, *22*, 8121−8126.
(5) Strother, T.; Knickerbocker, T.; Russell, J. N., Jr.; Butler, J. E.; Smith, L. M.; Hamers, R. J. *Langmuir* **2002**, *18*, 968−971.
(6) Nichols, B. M.; Butler, J. E.; Russell, J. N., Jr.; Hamers, R. J. *J. Phys. Chem. B* **2005**, *109*, 20938−20947.
(7) Baker, S. E.; Tse, K. Y.; Hindin, E.; Nichols, B. M.; Clare, T. L.; Hamers, R. J. *Chem. Mater.* **2005**, *17*, 4971−4978.
(8) Sun, B.; Colavita, P. E.; Kim, H.; Lockett, M.; Marcus, M. S.; Smith, L. M.; Hamers, R. J. *Langmuir* **2006**, *22*, 9598−9605.
(9) Yang, W. S.; Auciello, O.; Butler, J. E.; Cai, W.; Carlisle, J. A.; Gerbi, J.; Gruen, D. M.; Knickerbocker, T.; Lasseter, T. L.; Russell, J. N., Jr.; Smith, L. M.; Hamers, R. J. *Nat. Mater.* **2002**, *1*, 253−257.
(10) Yang, W.; Baker, S. E.; Butler, J. E.; Lee, C.-s.; Russell, J. N., Jr.; Shang, L.; Sun, B.; Hamers, R. J. *Chem. Mater.* **2005**, *17*, 938−940.
(11) Nichols, B. M.; Metz, K. M.; Tse, K. Y.; Butler, J. E.; Russell, J. N.; Jr.; Hamers, R. J. *J. Phys. Chem. B* **2006**, *110*, 16535−16543.
(12) Himpsel, F. J.; Knapp, J. A.; VanVechten, J. A.; Eastman, D. E. *Phys. Rev. B* **1979**, *20*, 624−627.
(13) Diederich, L.; Aebi, P.; Kuttel, O. M.; Schlapbach, L. *Surf. Sci.* **1999**, *424*, L314−L320.
(14) Ley, L.; Graupner, R.; Cui, J. B.; Ristein, J. *Carbon* **1999**, *37*, 793−799.
(15) Baumann, P. K.; Nemanich, R. J. *Surf. Sci.* **1998**, *409*, 320−335.
(16) van der Weide, J.; Zhang, Z.; Baumann, P. K.; Wensell, M. G.; Bernholc, J.; Nemanich, R. J. *Phys. Rev. B* **1994**, *50*, 5803−5806.

10.1021/ja073944y CCC: $37.00

Scheme 1

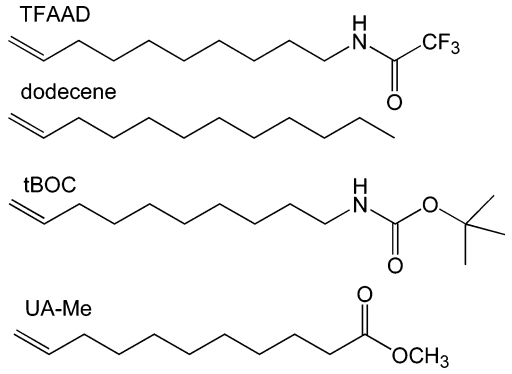

photoelectron injection (also known as internal photoemission) in the reactions of other forms of carbon and possibly even other materials has not been previously established. Amorphous carbon is an excellent candidate for these studies because in addition to being of great practical importance, its ability to be deposited on a range of substrates facilitates a variety of fundamental measurements of its chemical and photoelectrochemical properties.

Here, we report a detailed investigation on the mechanism of the photochemical grafting of *n*-alkenes on amorphous carbon thin films and on the factors governing the reaction yield. Using Infrared Reflectance Absorption Spectroscopy (IRRAS) and X-ray Photoelectron Spectroscopy (XPS) we compare the reactivity of *n*-alkenes of similar length, carrying different terminal functional groups. Our results show that there are pronounced differences in photochemical functionalization efficiency between different terminal alkenes. Using density functional calculations, we show that the reactivities of the four different molecules are highly correlated with their electron affinities, strongly suggesting that electron emission from the solid to the alkene plays the key role in the photochemical functionalization of amorphous carbon. Using this knowledge, we show that the grafting of low-reactivity molecules can be greatly enhanced by seeding with a small amount of a molecule bearing a good electron-accepting group, such as the trifluoracetamide group, at the distal end. These results provide important new insights into the role of electron ejection in the grafting of alkenes on surfaces and demonstrate how an understanding of the mechanism yields improved methods for controlled functionalization of the surfaces. While demonstrated here on surfaces of *amorphous* carbon, the results are expected to have broad applicability to a wider range of surfaces and may provide additional insights into the mechanism of photochemical grafting of alkenes on other sufaces.

2. Experimental Section

Chemicals. Absolute ethanol (Aaper), electronic grade methanol (Fisher), and chloroform (Fisher) were used without further purification. The following compounds were used for surface modification: 1-dodecene (Sigma), trifluoroacetic acid protected 10-aminodec-1-ene (TFAAD, Chemical Synthesis Services), 10-*N*-Boc-amino-dec-1-ene (tBOC, Astatech, Inc.), and methyl 10-undecenoate (UA-Me, Sigma). Scheme 1 shows the molecular structure of the alkenes. All of the compounds were used as neat liquids. The tBOC and TFAAD molecules were purified by vacuum distillation.

Substrate Preparation. Amorphous carbon films 50 nm thick were prepared by sputter-coating using a DC magnetron system (Denton Vacuum) with a base pressure of 2×10^{-6} Torr or lower and an Ar pressure of 3 mTorr. The films were sputtered on different types of substrates according to the requirements of each characterization technique: glass slides for photocurrent measurements, polished glassy carbon plates for electrochemical measurements, 100 nm evaporated titanium films on glass slides or silicon wafers for IRRAS measurements, and Ti-coated Mo foils for XPS and UPS. The use of titanium resulted in excellent adhesion of the carbon film to the substrates and also served as a metal substrate to enhance the IRRAS signal. The amorphous carbon films were hydrogen-terminated in a 13.56 MHz inductively coupled plasma, at a H_2 pressure of 10 Torr, for 10 min.

Photochemical Functionalization. The H-terminated amorphous carbon samples were placed inside a nitrogen-purged reaction chamber sealed with a quartz window. A few drops of the neat alkene compound were placed on the substrates, and a quartz slide was placed over the liquid to prevent evaporation. The cell was illuminated with a low-pressure mercury lamp (254 nm, 4.9 eV photon energy). The samples were then rinsed using chloroform, ethanol, and methanol and finally dried under a nitrogen flow.

Density Functional Calculations. The electronic energies, zero-point energies, equilibrium structures, and vibrational frequencies were calculated for the four unsaturated neutral alkenes and their radical anions and cations, using density functional theory methods (DFT) and the Gaussian03 set of programs.[17] We used Becke's three-parameter hybrid exchange functional[18] with the Lee, Yang, and Parr's correlation functional[19] (B3LYP). We used the built-in Dunning/Huzinaga D95 full double-ζ basis set[20] and performed geometry optimization and vibrational energy calculations with it.

Adiabatic IPs and EAs were calculated according to

$$\begin{aligned} \mathrm{EA} &= E(\text{optimized neutral}) - E(\text{optimized anion}) \\ \mathrm{IP} &= E(\text{optimized cation}) - E(\text{optimized neutral}) \end{aligned} \quad (1)$$

Vibrational energies were added to the electronic energies in order to obtain the electron affinities and ionization potentials corrected by the zero-point energy (ZPE) differences between the neutral and the ionic species (EA_{ZPE} and IP_{ZPE}, respectively).

Previous studies of molecular adsorbates,[21−23] and electron attachment experiments,[24,25] have sometimes found improved agreement between experimental and calculated values using vertical electron affinity (VEA) because electron attachment/detachment is fast compared with nulcear motion. Consequently, we also calculated vertical electron affinities (VEAs) and the vertical ionization potentials (VIPs), defined as the energy change associated to the instantaneous attachment (VEA) or detachment (VIP) of an electron from the neutral molecule, prior to any relaxation of the nuclear coordinates. These were calculated using

$$\begin{aligned} \mathrm{VEA} &= E(\text{optimized neutral}) - E(\text{anion at optimized neutral coordinates}) \\ \mathrm{VIP} &= E(\text{cation at optimized neutral coordinates}) - E(\text{optimized neutral}) \end{aligned} \quad (2)$$

Characterization. Infrared reflection−absorption spectra were collected on a Bruker Vector 33 FTIR spectrometer equipped with a VeeMaxII variable angle specular reflectance accessory and a wire grid polarizer. The presence of a metal underlayer (100 nm Ti) enhanced the reflectance of the sample and controlled the surface selection rules,

(17) Frisch, M. J., et al. Gaussian, Inc.: Wallingford, CT, 2004.
(18) Becke, A. D. *Phys. Rev. A* **1988**, *38*, 3098−3100.
(19) Lee, C.; Yang, W.; Parr, R. G. *Phys. Rev. B* **1988**, *37*, 785−789.
(20) Dunning, T. H., Jr.; Hay, P. J. In *Modern Theoretical Chemistry*; Schaefer, H. F., III, Ed.; Plenum: New York, 1976; Vol. 3.
(21) Kasemo, B. *Surf. Sci.* **1996**, *363*, 22−28.
(22) Zhu, X. Y. *Annu. Rev. Phys. Chem.* **1994**, *45*, 113−144.
(23) Lee, J.; Ryu, S.; Ku, J. S.; Kim, S. K. *J. Chem. Phys.* **2001**, *115*, 10518−10524.
(24) Modelli, A.; Jones, D. *J. Phys. Chem. A* **2004**, *108*, 417−424.
(25) Modelli, A.; Venuti, M. *J. Phys. Chem. A* **2001**, *105*, 5836−5841.

which were analogous to those found for metal substrates.[26] Spectra were collected using p-polarized light at 80° incidence from the surface normal; 500 scans at 4 cm^{-1} resolution were collected for both background and sample. The spectra were baseline-corrected and offset for clarity. Typical rms and peak-to-peak noise levels in the spectra were below 2×10^{-5} and 1×10^{-4} absorbance units, respectively.

XPS characterization was performed on an ultrahigh vacuum system, with a base pressure of 8×10^{-10} Torr, equipped with a monochromatized Al K_α source (1486.6 eV), and a multichannel array detector. Spectra reported here were recorded with an analyzer resolution of 0.1−0.2 eV at a 45° takeoff angle. Atomic area ratios were determined by fitting the raw data to Voigt functions (Igor Pro) after Shirley background correction[27] and normalizing the peak area ratios by the corresponding atomic sensitivity factors (C = 0.296; N = 0.477; O = 0.711; F = 1.0). UPS characterization was carried out using a He(I) emission lamp (21.2 eV) as an excitation source and an analyzer resolution of 0.05−0.1 eV. Samples were collected at a takeoff angle of 75° (from the surface plane) and biased −4.50 to −8.00 V with respect to the spectrometer to ensure that the vacuum level of the sample was higher in energy than that of the analyzer. Spectra at progressively higher biases were collected until the high binding energy cutoff was observed to converge; the spectrum obtained at the bias at which convergence was observed was used for the work function calculations. Energies are referenced to the sample Fermi level, which was determined by measurement of Ta clips directly in contact with the sample.

Electrical properties of hydrogen terminated surfaces were characterized using AC-impedance spectroscopy in a three-electrode cell using amorphous carbon films deposited on glassy carbon plates as the working electrode. A Viton O-ring pressing against the working electrode limited the exposed area to 0.036 cm^2; all of the reported experimental data were area-normalized to this value. The counter-electrode was a Pt foil, and the reference electrode was a Ag/AgCl/3 M KCl electrode (Cypress Systems). Measurements were performed at room temperature in KCl solutions of 0.01, 0.1, and 1 M concentrations purged with Ar before and during the experiments. Impedance data were collected using a potentiostat (Solartron 1287) and an impedance analyzer (Solartron 1260) with Zplot software (Scribner Associates, Inc.).

3. Results

Influence of Molecular Structure on Rate of Photochemical Functionalization. The hydrogen-terminated carbon surfaces were covered by a thin film of different liquid alkenes and illuminated with 254 nm light. Scheme 1 shows the four alkenes used; all have similar carbon chain lengths and have terminal alkene groups but differ in the functional group at the distal end. Typical experiments used an illumination time of 15 h, based on measurements of the reaction yields (*vide infra*). Control experiments showed that UV light was required in order to obtain any monolayer coverage on the carbon surfaces (see Supporting Information). The organic layers obtained in this way were characterized via IRRAS spectroscopy and, in the case of TFAAD, also via XPS.

Figure 1 shows IRRAS spectra of the organic layers obtained after photochemical grafting for 15 h on hydrogen-terminated surfaces. The infrared spectra of the four alkenes have been discussed in previous work;[8,28] reference solution spectra and details about peak assignments can be found in the Supporting Information. It is evident that the infrared absorbances are remarkably different for different alkenes. Since all of the molecules investigated here have the same number of methylene units along their backbone except for dodecene, which has one more, as a first approximation, the intensity associated with the CH_2 peaks (∼2930 and ∼2858 cm^{-1}) would be expected to be similar if they displayed similar surface densities. Small variations in peak intensity could be attributed to molecular orientation effects; however, the large differences in intensity observed after the same reaction times for the various alkenes strongly suggest differences in final coverage. The net absorbances of the $-CH_2$ asymmetric stretching, therefore, offer a useful qualitative means of estimating the monolayer coverage; dodecene was found to be almost completely unreactive, and both UA-Me and tBOC layers yielded only ∼10% of the coverage obtained for TFAAD.

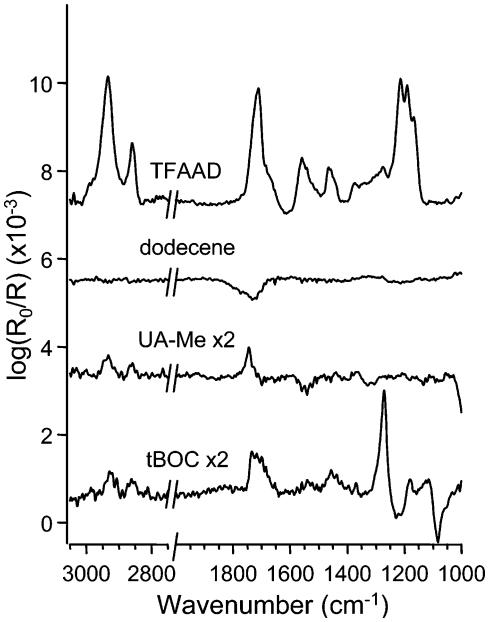

Figure 1. IRRAS spectra of the organic layers obtained for different alkene molecules on H-terminated surfaces after 15 h illumination time. Spectra were baseline corrected and offset for clarity. TFAAD is the alkene that yields the highest coverage; tBOC and UA-Me appear to graft only with small coverage whereas dodecene is completely unreactive.

The terminal group on TFAAD contains fluorine atoms, facilitating quantitative characterization of the molecular layer using XPS. To characterize the kinetics of TFAAD grafting, we monitored the $A_{F(1s)}/A_{C(1s)}$ ratio as a function of illumination time. Figure 2a shows the evolution of the $A_{F(1s)}/A_{C(1s)}$ ratio for the reaction carried out on the H-terminated surface. The surface coverage reaches a plateau after approximately 4 h, when the $A_{F(1s)}/A_{C(1s)}$ ratio becomes close to the final value of 0.20 ± 0.01 achieved after 15 h. However, use of the $A_{F(1s)}/A_{C(1s)}$ ratio as a measure of surface coverage is error-prone on carbon substrates because of the difficulty of distinguishing C(1s) signals from the molecular layer and the underlying substrate.[29]

IRRAS was used as a complementary technique in order to characterize the time evolution of TFAAD layers. Figure 2b shows the integrated intensities in the C−H (∼2810−3040 cm^{-1}) and C═O stretching regions (∼1640−1830 cm^{-1}) as a function of illumination time. The intensities increase as a

(26) Tolstoy, V. P.; Chernyshova, I.; Skryshevsky, V. A. *Handbook of Infrared Spectroscopy of Ultrathin Films*; Wiley-VCH: Hoboken, NJ, 2003.
(27) Shirley, D. A. *Phys. Rev. B* **1972**, *5*, 4709−4714.
(28) Baker, S. E.; Colavita, P. E.; Tse, K. Y.; Hamers, R. J. *Chem. Mater.* **2006**, *18*, 4415−4422.
(29) Yang, N.; Uetsuka, H.; Watanabe, H.; Nakamura, T.; Nebel, C. E. *Chem. Mater.* **2007**, *19*, 2852−2859.

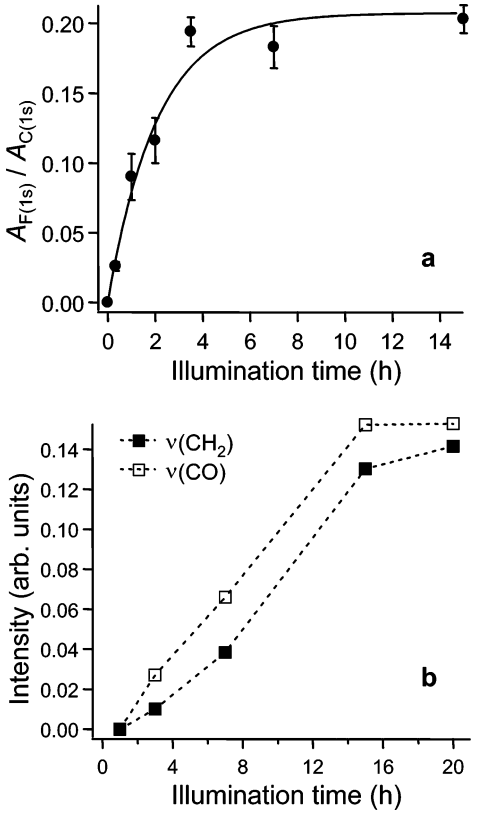

Figure 2. Reaction rate of TFAAD on hydrogen terminated amorphous carbon surfaces. (a) The reaction progress can be followed via XPS by calculating the $A_{F(1s)}/A_{C(1s)}$ as a function of reaction time. A weighed exponential fit has been added to the graph to guide the eye. The layer appears to self-terminate after approximately 4 h. (b) The integrated intensities of the C—H (■) and C═O (□) stretching peaks in IRRAS data were used as a complementary method to follow the progress of the reaction on H-terminated surfaces. The IRRAS results also show that the reaction plateaus after 15 h.

function of time and reach a plateau after 15 h of illumination, therefore suggesting that self-termination occurs at times >15 h. After 20 h of illumination (not shown), the onset of a slower grafting process is observed using IRRAS; we have therefore limited our characterization to layers grafted for 15 h or less.

These IRRAS data demonstrate that the yield of the photochemical reaction is highly dependent on the specific terminal group attached to the *n*-alkene. This observation is in stark contrast to previous mechanistic and kinetic studies on the photochemical grafting of *n*-alkenes on Si, where no differences or much smaller differences in reaction yield have been observed for molecules bearing various terminal groups.[30−32] In the case of TFAAD both XPS and IRRAS data indicate that the reaction is self-terminating.

Electronic Properties of the Amorphous Carbon Surfaces. The bulk properties of sputtered amorphous carbon films used in this work have been described previously.[8] The carbon is >85% in the sp^2-hybridized form, with no significant amounts of nitrogen or hydrogen detected by XPS or FTIR. Since the electronic properties are important for understanding its surface photochemical reactions, we characterized the surface composition and the valence band properties using XPS and UPS before and after brief exposure to a weak hydrogen plasma. The Supporting Information contains data and an expanded discussion of the XPS and UPS characterization of the as-deposited samples before hydrogen termination. Figure 3 shows XPS spectra of the C(1s) and O(1s) regions of the amorphous carbon film after hydrogen termination. The only elements present in the XPS survey scan were oxygen and carbon. The $A_{O(1s)}/A_{C(1s)}$ ratio was determined to be 0.055; this value is much lower than the oxygen content observed in as-deposited samples (typically >0.090). The C(1s) spectra of the H-terminated samples show an asymmetric broad line characteristic of amorphous carbon.[33,34] The spectrum was fitted with four components, centered at 283.8, 284.5, 285.3, and 287.6 eV. The first two peaks are separated by 0.7 eV, which is consistent with the separation between sp^2 and sp^3 carbon in disordered graphite and other amorphous carbon samples.[33,34] However, the intensities of these two components are highly correlated in the fit landscape, and determining the percent composition of these two phases is challenging. The two components at higher binding energy can be attributed to the presence of small amounts of oxidized carbon species, most likely in the subsurface region that is detected by XPS but not readily reduced by the H-plasma.

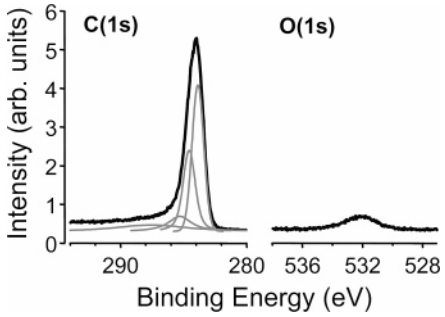

Figure 3. XPS in the C(1s) and O(1s) regions of sputtered amorphous carbon after hydrogen plasma treatment. The individual contributions to the C(1s) peak were obtained via fitting procedures and are reported under the curves.

Previous studies on the photochemical grafting of alkenes on diamond showed that the reaction was initiated by photoejection of electrons into the liquid alkene and proposed that these liquid-phase radicals abstracted H atoms from the surface to create surface sites that could then form covalent bonds with other liquid-phase alkenes to functionalize the surface.[6,11] Since the electronic structure of the surface is important for photoemission, we characterized the electronic structure of the amorphous carbon surface using UPS.

Figure 4 shows the He(I) UPS spectrum of a H-terminated amorphous carbon sample. The UPS profile is markedly different from that of the as-deposited sample (see Supporting Information), showing a single broad peak with maximum intensity at approximately 8.1 eV. This feature can be clearly assigned to the p-σ orbitals; the 8.1 eV value is similar to the 8.4 eV value previously observed for p-σ band emission on nanocrystalline hydrogen-terminated diamond.[6] The region near the Fermi energy does not show any notable features. No significant emission intensity is observed at energies between the Fermi energy and ~0.5 eV binding energy, consistent with

(30) Barrelet, C. J.; Robinson, D. B.; Cheng, J.; Hunt, T. P.; Quate, C. F.; Chidsey, C. E. D. *Langmuir* **2001**, *17*, 3460−3465.
(31) Liu, Y.-J.; Navasero, N. M.; Yu, H.-Z. *Langmuir* **2004**, *20*, 4039−4050.
(32) Faucheux, A.; Gouget-Laemmel, A. C.; Villeneuve, C. H. d.; Boukherroub, R.; Ozanam, F.; Allongue, P.; Chazalviel, J.-N. *Langmuir* **2006**, *22*, 153−162.
(33) Haerle, R.; Riedo, E.; Pasquarello, A.; Baldereschi, A. *Phys. Rev. B* **2001**, *65*, 045101−9.
(34) Jackson, S. T.; Nuzzo, R. G. *Appl. Surf. Sci.* **1995**, *90*, 195−203.

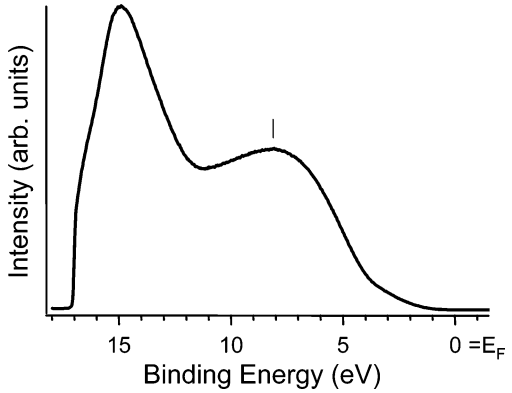

Figure 4. He(I) UPS spectrum of the hydrogen terminated sample. A linear extrapolation of the sharp threshold at high binding energy to zero intensity gives the surface work function. The prominent feature at 8.1 eV assigned to the p-σ states is indicated with a line.

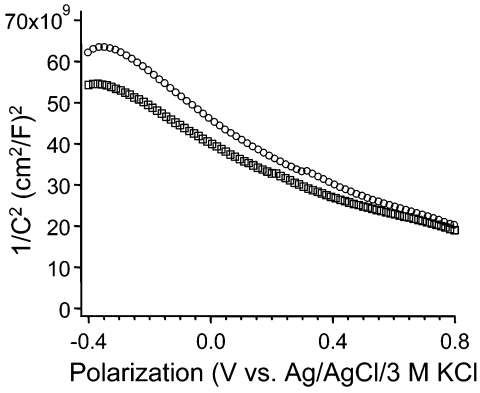

Figure 5. Mott−Schottky plots obtained for the H-terminated sample in 0.01 (○) and 0.1 M (□) KCl solutions at 10 Hz. The negative slope in the Mott−Schottky plots suggests p-type semiconducting behavior.

previous studies.[35] No significant changes were observed in the region near E_F when comparing the hydrogen-terminated to the freshly deposited sample.

To measure the work function, the sharp cutoff in electron emission at high binding energy was fit to a line and extrapolated to find the high binding-energy cutoff; this value was then subtracted from the incident photon energy (21.2 eV) to yield the work function.[36,37] This procedure resulted in a work function of 4.0 eV for the hydrogen-terminated sample, significantly lower than the value 4.8 eV found for the as-deposited sample (see Supporting Information). A work function of 4.0 eV after hydrogen termination is similar to work functions in the range 3.7−4.2 eV previously reported for hydrogen terminated diamond.[6,38] The decrease in work function produced by H-termination of the sample is consistent with previous studies showing that hydrogen termination lowers the work function of other carbon based materials such as diamond,[38] fullerenes, nanotubes, and graphite[39] due to the introduction of C−H surface dipoles in which the hydrogen positive charge is on the vacuum side of the interface.

The most important result from these UPS measurements is that the H-terminated samples have a work function of 4.0 eV that is substantially below the 4.9 photon energy used in the functionalization reactions. This result shows that illumination of the samples with 4.9 eV photons (254 nm) in a vacuum will result in the ejection of photoelectrons. However, since electrons in a fluid are expected to be stabilized by dielectric polarization,[40] these results also imply that photoelectron ejection should be expected into the organic alkenes.

In agreement with previous studies,[41] the carbon surfaces contain a mixture of sp^3- and sp^2-hybridized carbon in which the π states associated with the sp^2-hybridization dominate the density of states nearest the Fermi energy. The low density of states near E_F gives rise to semiconducting behavior that was also characterized by measuring the interfacial impedance of the amorphous carbon samples in contact with aqueous solutions of KCl, using impedance spectroscopy. We first verified that the interfacial impedance was independent of the KCl concentration by performing impedance measurements as a function of frequency for three different concentrations of KCl: 0.01, 0.1, and 1 M. The impedance spectra were collected by applying a sinusoidal potential at frequencies ranging from 0.1 to 10^5 Hz and with an amplitude of 10 mV centered at 0.40, 0.36, and 0.28 V vs Ag/AgCl/3 M KCl (open circuit potentials) for 0.01, 0.1, and 1 M concentrations, respectively. A more detailed discussion of these results can be found in the Supporting Information. We extracted the interfacial capacitance as a function of KCl concentration by fitting the impedance to the Randles model,[42] yielding values of 5.4, 4.8, and 5.0 μF/cm^2 for the 0.01, 0.1, and 1.0 M KCl concentrations, respectively. The lack of sensitivity to KCl concentration shows that the interfacial capacitance is dominated by the space-charge layer of the amorphous carbon surface (at the potentials used in our measurements) and not by the electrical double-layer at the carbon−electrolyte interface.[43] The resulting value of ~5 μF/cm^2 is lower than that of glassy carbon (13 μF/cm^2)[44] and higher than that of H-terminated diamond (3.04 μF/cm^2),[45] again suggesting a density of states intermediate between that of a wide-band gap semiconductor (diamond) and a good metal (glassy carbon). This in turn implies that the H-terminated amorphous samples are semiconducting. Figure 5 shows Mott−Schottky plots collected in 0.01 and 0.1 M KCl solution at 10 Hz. The capacitance used for these plots was extracted from the impedance data by modeling the interface as a series RC circuit (a plot of the capacitance as a function of polarization can be found in the Supporting Information). The curve shows a decrease in $1/C^2$ with an increasingly positive potential, which is characteristic of a p-type semiconductor.[46] Both concentrations show a broad negative slope, indicating that the amorphous carbon electrode behaves as a p-type semiconductor. The curvature of the Mott−Schottky plots suggests the presence of

(35) Mansour, A.; Ugolini, D. *Phys. Rev. B* **1993**, *47*, 10201−10209.
(36) Schlaf, R.; Schroeder, P. G.; Nelson, M. W.; Parkinson, B. A.; Lee, P. A.; Nebesny, K. W.; Armstrong, N. R. *J. Appl. Phys.* **1999**, *86*, 1499−1509.
(37) Ertl, G.; Küppers, J. *Low Energy Electrons and Surface Chemistry*; Wiley-VCH: Weinheim, 1986.
(38) Diederich, L.; Küttel, O. M.; Aebi, P.; Schlapbach, L. *Surf. Sci.* **1998**, *418*, 219−239.
(39) Ruffieux, P.; Gröning, O.; Bielmann, M.; Mauron, P.; Schlapbach, L.; Gröning, P. *Phys. Rev. B* **2002**, *66*, 245416.
(40) Born, M. *Z. Physik A* **1920**, *1*, 45−48.
(41) Robertson, J. *Philos. Mag. B* **1992**, *66*, 199−209.
(42) Randles, J. E. B. *Discuss. Faraday Soc.* **1947**, *1*, 11−19.
(43) Bard, A. J.; Faulkner, L. *Electrochemical Methods: Fundamentals and Applications*, 2nd ed.; J. Wiley: New York, 2001.
(44) Randin, J. P.; Yeager, E. *J. Electroanal. Chem. Interfacial Electrochem.* **1975**, *58*, 313−322.
(45) Tse, K.-Y.; Nichols, B. M.; Yang, W.; Butler, J. E.; Russell, J. N., Jr.; Hamers, R. J. *J. Phys. Chem. B* **2005**, *109*, 8523−8532.
(46) Memming, R. *Semiconductor electrochemistry*; Wiley-VCH: Weinheim, 2001.

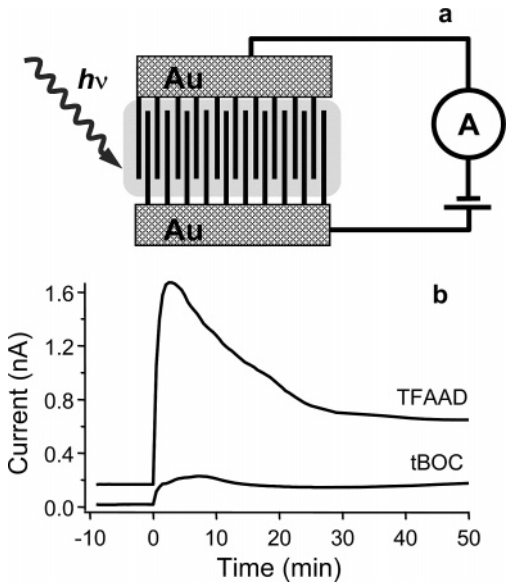

Figure 6. Photocurrent measurements carried out using interdigitated electrodes covered by a thin film of the liquid alkene. (a) Schematics of the experimental setup used in the measurements where $h\nu = 4.9$ eV. (b) Current profiles for TFAAD and tBOC, where $t = 0$ is the time at which illumination started.

midgap states[47−50] and makes it difficult to establish a flatband potential.

In summary, both UPS and impedance measurements revealed that the H-terminated amorphous carbon is a semiconductor. The UPS measurements show that the valence band onset (likely arising from π states of the film) is located at ∼0.5 eV below E_F. The impedance data show that the overall behavior is that of a p-type semiconductor; since the UPS data show the valence band onset at ∼0.5 eV below E_F, this implies that the conduction band must lie at least 0.5 eV above E_F, although there are states within the gap as well.

Role of Photoelectron Emission at the Carbon/Liquid Interface. The UPS data show that the 4.9 eV photons used in our photochemical reaction should be sufficient to eject photoelectrons into a vacuum. However, the grafting reaction takes place at the carbon/liquid interface where the barriers to photoejection might be very different from those measured under ultrahigh vacuum conditions. Also, these barriers to electron emission might be different in the four different alkenes used in our experiments. In order to investigate whether electron emission takes place at this interface under illumination using 4.9 eV photons, we carried out photocurrent measurements using interdigitated carbon electrode arrays.

Figure 6a shows a schematic of the setup used for the experiments. Amorphous carbon was deposited onto glass substrates using a photoresist mask to produce interdigitated electrodes 0.5 mm wide, with 0.5 mm gaps between electrodes. A small drop of liquid alkene was placed on the electrodes and a UV-transparent quartz slide then covered the sample, forming a thin liquid layer ∼20 microns thick. A bias voltage of 0.04 V was applied to the electrodes, and the current was allowed to stabilize for at least 2 h in the dark in an argon atmosphere prior to any measurements. Figure 6 shows typical current profiles for TFAAD (trace A) and tBOC (trace B) on hydrogen-terminated electrodes where $t = 0$ is the time at which the UV illumination begins. In both cases, UV illumination causes a rapid increase in current, followed by a slower decay to a steady-state value of ∼0.65 nA (TFAAD) and ∼0.15 nA (tBOC). Control experiments using a saturated molecule, dodecane, under the same conditions showed much smaller photocurrents, in the range 1−3 pA.

UV−visible absorption spectra of the two alkenes show very low absorptions at 254 nm for both TFAAD and tBOC; this indicates that bulk ionizations do not contribute to the measured currents and that currents generated by the UV light must be due to charge separation occurring at the electrode/liquid interface. The observed peak photocurrents are more than 7 times larger for TFAAD than for tBOC, and at steady state the two photocurrents still differ by a factor of ∼4. Assuming that both liquids are similar in nature, this finding suggests that any photoinduced charge-transfer process is more efficient for TFAAD than for tBOC.

Similarly to the case of TFAAD on diamond surfaces, the reaction of alkenes on amorphous carbon therefore appears to be photoelectrochemical in nature.[11] Assuming to a first approximation that the collection of charged species in the two liquids is equal, the observed photocurrent magnitudes appear to reflect the reaction yield, thus indicating that the efficiency with which charge transfer takes place at the carbon/liquid interface correlates with the alkene grafting rate.

Theoretical Study of the Alkene Donor and Acceptor Levels. Our experimental results demonstrate that (1) there are remarkable differences in reactivity between alkenes bearing various terminal groups and (2) the grafting reaction on amorphous carbon involves electron emission from carbon into the alkene, similar to what had been reported for diamond substrates.[6,11] In the case of diamond, the proposed mechanism of photochemical grafting of terminal alkenes consists of an initiation followed by a propagation step. The initiation step involves photoemission of electrons into the liquid, producing anions that can abstract hydrogen from the diamond surface, thereby creating reactive "dangling bonds". Propagation can occur by reaction of these surface dangling bonds with a terminal olefin, yielding a surface bound radical species that can propagate the reaction.[51] The propagation step involves only the unsaturated C═C bond and is therefore expected to be independent of the terminal group. However, in the photochemical initiation step, the barriers to electron photoemission have been shown to play an important role in determining the reactivity of hydrogen- vs oxygen-terminated diamond.[6] Since the results of the present study indicate that the reaction on amorphous carbon is also photoelectrochemical, we conducted theoretical studies to understand the energy changes involved in charge transfer between the electrodes and the alkenes and how these depend on the nature of the alkene.

The propensity of oxidation vs reduction of the alkenes in solution by the amorphous carbon can be estimated by considering the relative energies of the amorphous carbon band edges and of the acceptor and donor levels in the liquid alkenes. In order to determine the donor and acceptor levels for the different

(47) Nogami, G. *J. Electrochem. Soc.* **1986**, *133*, 525−531.
(48) Morrison, S. R. *Electrochemistry at semiconductor and oxidized metal electrodes*; Plenum Press: New York, 1980.
(49) Dean, M. H.; Stimming, U. *J. Phys. Chem.* **1989**, *93*, 8053−8059.
(50) Dean, M. H.; Stimming, U. *J. Electroanal. Chem.* **1987**, *228*, 135−151.
(51) Cicero, R. L.; Chidsey, C. E. D.; Lopinski, G. P.; Wayner, D. D. M.; Wolkow, R. A. *Langmuir* **2002**, *18*, 305−307.

Table 1. Electron Affinities (EAs) and Ionization Potentials (IPs) Calculated Using the B3LYP Hybrid Functional and the D95 Basis Set[a]

	B3LYP/D95					
	EA	EA_{ZPE}	VEA	IP	IP_{ZPE}	VIP
dodecene	−2.29	−2.08	−2.64	8.49	8.40	8.75
tBOC	−1.59	−1.39	−2.05	8.02	7.97	8.19
UAMe	−1.15	−0.99	−1.48	8.43	8.38	8.59
TFAAD	0.03	0.16	−0.76	8.59	8.54	8.86

[a] EA_{ZPE} and IP_{ZPE} are the adiabatic EA and IP values calculated by including vibrational energy corrections to the electronic energies. VEA and VIP are the vertical EA and IP values, respectively. Values are in eV and were calculated using eqs 1 and 2 as described in the text.

alkenes, we carried out density functional calculations to obtain the energy of the neutral molecules and their respective unsaturated anion and cation species. DFT methods were chosen because they have been shown to provide excellent agreement with experimental values of EAs and IPs.[52,53]

The donor and acceptor level positions relative to those under vacuum in the gas phase were calculated from the ionization potentials (IPs) and the electron affinities (EAs), respectively. More positive EAs reflect easier reduction of the molecules, while more negative IPs indicate more facile oxidation. Table 1 summarizes the values thus obtained for the adiabatic EA and IP as well as the VEA and VIP for the four molecules used in our experimental studies. Very similar trends are observed using both vertical and adiabatic electron affinities and ionization potentials.

The first result that emerges from these calculations is that the EAs of the four alkenes span a wide range of energies, depending on the specific type of functional group at the α-terminus. In the case of the adiabatic affinities the highest singly occupied molecular orbital (SOMO) is strongly localized at the α-terminus, except in the case of dodecene, where it is localized on the olefin group. The unpaired spin density distributions, which provide a measure of the localization of unpaired electrons on molecules,[54,55] also indicate that the terminal group is important for accommodating the excess electron. In the case of the vertical affinities, the spin density becomes progressively more localized at the terminal group opposite the olefin as the EA becomes more positive. The spin density in dodecene is strongly localized at the C═C bond, whereas that of TFAAD is strongly localized at the trifluoroacetamide group; tBOC and UA-Me present an intermediate case. In the relaxed anion calculations (adiabatic EA), the spin densities indicate that the unpaired electron is even more localized at the α-terminus for all of the alkenes (except for dodecene) strongly suggesting that the α-terminus is of great consequence for the stability of the anion (see Supporting Information).

In contrast, the ionization potentials are all clustered very close in energy for all four molecules, and the HOMO orbitals of the neutral molecules are strongly localized on the alkene group, except for tBOC. In the latter case, the HOMO orbital is localized on the carbamate group.

(52) Rienstra-Kiracofe, J. C.; Tschumper, G. S.; Schaefer, H. F., III; Nandi, S.; Ellison, G. B. *Chem. Rev.* **2002**, *102*, 231−282.
(53) Curtiss, L. A.; Redfern, P. C.; Raghavachari, K.; Pople, J. A. *J. Chem. Phys.* **1998**, *109*, 42−55.
(54) Pople, J. A.; Beveridge, D. L.; Dobosh, P. A. *J. Am. Chem. Soc.* **1968**, *90*, 4201−4209.
(55) Brinkmann, N. R.; Schaefer, H. F., III; Sanderson, C. T.; Kutal, C. *J. Phys. Chem. A* **2002**, *106*, 847−853.

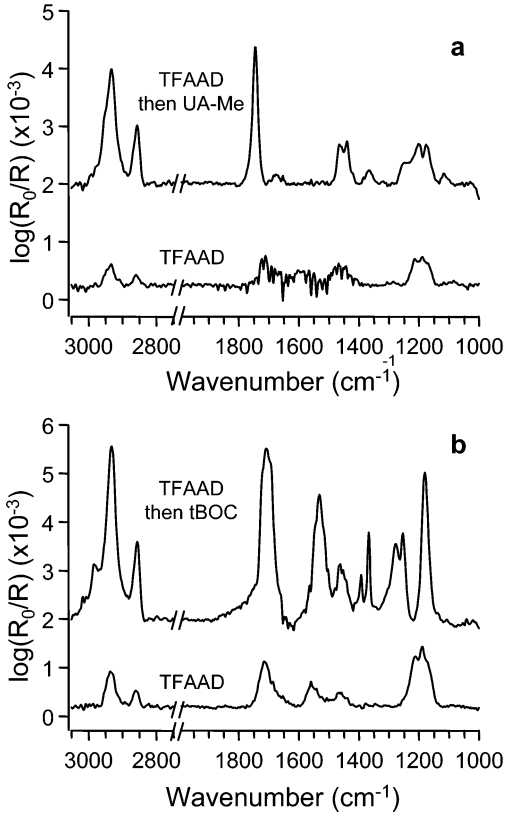

Figure 7. IRRAS spectra of (a) UA-Me and (b) tBOC layers obtained after 15 h illumination time, on a TFAAD-seeded surface. Spectra were baseline corrected and offset for clarity. The a-C surfaces were H-terminated and pregrafted with a TFAAD to approximately 50% coverage. tBOC and UA-Me graft only in traces on the bare H-terminated surface but graft to high coverages on the TFAAD seeded surface.

A second important result is that the EA values, both vertical and adiabatic, follow the trends in reactivity: the acceptor level of TFAAD is lowest in energy, followed by tBOC and UA-Me, with dodecene being the highest. The strong correlation between the electron affinities and the observed reactivities strongly suggests that the functionalization reaction requires the injection of an electron into the acceptor level of the alkene, in analogy to what had been observed for diamond.[11] Since the acceptor level is highly dependent on the specific terminal group, the reactivity of each molecule can be remarkably different.

Enhancement of the Reactivity by Surface "Seeding" with an Initiator. Our IRRAS results show that TFAAD compared to other alkenes displays a much higher reactivity on H-terminated amorphous carbon films. EA and IP calculations at the DFT level of theory showed that the reactivity of the molecules correlates closely with the ability of the terminal group at the α-terminus to function as a good electron acceptor. This suggests that the electron-accepting ability of TFAAD might be used as a way of enhancing the grafting of other molecules by having a small amount of TFAAD on the surface. Our hypothesis was that a good initiating group at the surface could create a reactive site for the radical addition to an olefin moiety of a second alkene. To test this hypothesis, we pregrafted a partial TFAAD layer, of approximately 20−50% coverage, and investigated how this affected the subsequent grafting of tBOC and UA-Me on H-terminated amorphous carbon.

Figure 7 follows the evolution of the IRRAS spectrum for two samples that were both pregrafted with a TFAAD layer for

Table 2. Peak Frequencies and Assignments for the IRRAS Spectra of TFAAD, tBOC, and UA-Me Layers[a]

	peak positions (cm^{-1})		
assignments[a]	TFAAD	tBOC	UA-Me
$\nu(CH_3)$ a	-	2983	sh
$\nu(CH_2)$ a	2934	2931	2931
$\nu(CH_2)$ s	2859	2856	2856
ν(C═O)	1711	1709	1743
β(NH) ν(CN) ν(CC)	1558	1531	-
$\beta(CH_2)$	1466	1462	1466
$\beta(CH_3)$	-	1392	1440
		1367	1367
ν(C—O)	-	1180	1201
			1178
ν(C—F)	1213	-	-
	1190		
	1167		

[a] ν = stretching; β = bending; a = asymmetric; s = symmetric.

a short time (1.3 h) and then rinsed and dried. One sample was then covered with pure tBOC (Figure 7a) and the second was covered with pure UA-Me (Figure 7b), before illumination for 15 h. The resulting infrared spectra show intense peaks at the characteristic positions for both tBOC and UA-Me layers (see Table 2 for peak positions and assignments).[8,28] The C═O stretching modes of the carbamate and ester moieties appear at 1709 and 1743 cm^{-1}, respectively; the peaks associated with —CH_3 vibrations are evident in the stretching region of the tBOC spectrum (~2983 cm^{-1}) and in the bending region (1440−1360 cm^{-1}) for both tBOC and UA-Me.[28] The vibrations associated with the —CH_2 stretchings (2931 and 2956 cm^{-1}) increase in intensity when compared to the initial net absorbances of the "seed" TFAAD layer; the calculated net absorbance for the peak positioned at 2931 cm^{-1} increases by a factor of ~5 in both cases. The final intensities of the tBOC and UA-Me layers are comparable to those of a TFAAD layer obtained after 15 h of illumination, indicating that the grafting of these two alkenes occurs with high efficiency on the samples pregrafted with TFAAD. Furthermore, the peaks at 1213, 1190, and 1167 cm^{-1} that are characteristic of the TFAAD —CF_3 group (see Table 2) disappear. Thus, we conclude that (1) TFAAD enhances the grafting of tBOC and UA-Me on the surface and (2) the grafting of tBOC and UA-Me replaces the TFAAD that was present initially.

The presence of TFAAD bonded to the carbon surface, therefore, enhances the yield of the photochemical grafting reaction for other alkenes. This behavior is consistent with our theoretical calculations, which showed that the ability of TFAAD to function as a good initiator for the reaction correlates with its good electron-accepting properties, and that the trifluoroacetamide terminal group is the moiety responsible for these properties. The initial grafting of a partial layer of TFAAD places good initiating groups (trifluoroacetamides) in close proximity to the surface, so that they can serve to create binding sites in order for the second alkene to graft through its olefin terminal group. Based on the net absorbance of the CH_2 asymmetric stretching peak, the observed final coverage of the second alkene is approximately 5 times higher than that of the initial TFAAD layer for both alkenes shown in Figure 7. Thus, more than one molecule of the second alkene is grafted for each trifluoroacetamide group located at the surface, suggesting that the reaction proceeds via a radical mechanism in which a single initiating species is responsible for multiple grafting events.

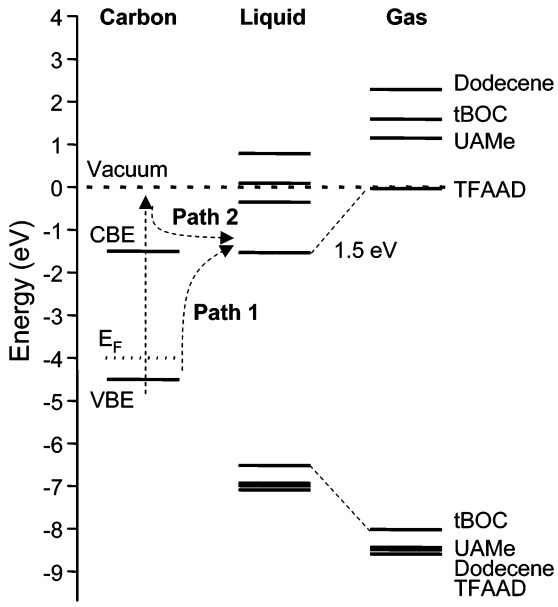

Figure 8. Energy level diagram showing estimated positions of the carbon valence and conduction band edges (VBE and CBE, respectively), and the calculated positions of acceptor and donor levels of the alkenes in liquid and gas phase. The polarization shift of 1.5 eV of the alkene levels was estimated from tabulated values of polarization energies of hydrocarbons. The conduction edge position was also estimated from previously reported values of amorphous carbon bandgaps. Two possible pathways, Path 1 and Path 2 for the initiation mechanism, are discussed in the text.

4. Discussion

While UV light can induce many surfaces (including silicon,[1,2,56,57] germanium,[3] gallium nitride,[4] and diamond)[5,6] to react with alkenes, many mechanistic aspects of the functionalization reactions remain poorly understood, and it is not clear whether different materials react via different mechanistic pathways. Recent work in our group[6,11] showed that on hydrogen-terminated diamond, alkenes are covalently linked to the diamond through a photoelectrochemical radical mechanism. The reaction consists of two discrete steps: (a) an initiation step in which radical anion species, generated via photoemission of electrons into the liquid alkene phase, create dangling bonds at the diamond surface by abstraction of hydrogen from the H-terminated surface; (b) subsequent addition reaction of these surface radicals to olefin terminal groups. Since diamond and amorphous carbon are both carbon based materials but have very different structures and electronic properties, it is useful to use the established diamond mechanism as a working hypothesis to investigate the mechanism on hydrogen-terminated amorphous carbon films.

Electronic Structure of the Carbon−Alkene Interface. Before explicitly addressing the mechanism, we first discuss the overall electronic structure of the carbon−alkene interface as gleaned from the DFT calculations and photoemission experiments. Figure 8 summarizes these results. The left side of Figure 8 shows a schematic of the electronic structure of hydrogen terminated carbon, where the zero in energy scale is the vacuum level. The work function is defined as the difference between the Fermi energy in the material (E_F) and the vacuum level, so that $E_F = -4.0$ eV in our scale. It is difficult to

(56) Langner, A.; Panarello, A.; Rivillon, S.; Vassylyev, O.; Khinast, J. G.; Chabal, Y. J. *J. Am. Chem. Soc.* **2005**, *127*, 12798−12799.
(57) Stewart, M. P.; Buriak, J. M. *J. Am. Chem. Soc.* **2001**, *123*, 7821−7830.

determine exactly the band edges in amorphous carbon due to the high density of mid-gap states. However, our UPS data show that there is a significant density of occupied electronic states starting from ~0.5 eV below E_F. This valence edge is indicated as VBE in our diagram. Our impedance spectroscopy data, however, show that hydrogen-terminated carbon behaves as a p-type semiconductor, suggesting that the conduction band minimum should be positioned at least 0.5 eV above E_F in order to yield p-type behavior. In Figure 8 we have chosen a somewhat arbitrary value of 3 eV for our band gap, which is at the high end of the 0.5−3.0 eV band gap range typically reported in the literature.[58,59] We emphasize that the exact value of the band gap and position of the conduction band do not have any significant impact on the interpretation of our results. This approximate conduction band edge (CBE) is labeled in Figure 8.

The far right side of Figure 8 shows the calculated donor and acceptor levels for the four alkenes used in our experiments, obtained by taking the negative of the adiabatic ionization energies and of the adiabatic electron affinities, respectively. This figure uses the adiabatic values without vibrational energy corrections. However our calculations show that the use of vertical energies (VEA and VIP) or the inclusion of vibrational energy corrections yield very similar results. The center of Figure 8 shows estimated values for donor and acceptor levels after polarization of the surrounding medium, which stabilizes both cations and anions. Typical values of the polarization energy (sometimes referred to as the Born energy)[40] are between 1 and 3 eV depending on the dielectric constant of the liquid and the ionic radius of the ion.[60] A value of ~1.5 eV for the polarization energy of saturated and unsaturated hydrocarbons is typical based on polarization energies determined from photoionization experiments.[61] The center panel of Figure 8 uses this 1.5 eV shift for all four molecules.

It is notable that all four molecules have very low-energy donor states that lie well below the valence band of the amorphous carbon. The similarity in energy of these donor states suggests that all four molecules should show similar rates for oxidation reactions, while their very low energy indicates that oxidation could only be thermodynamically possible via creation of very deep-lying holes in the amorphous carbon. In contrast, the acceptor states are significantly closer to the conduction band and change in a manner that correlates with the observed changes in reactivity: TFAAD shows the highest electron affinity (i.e., lowest-lying acceptor level) and is the most reactive of the molecules.

Role of Photoelectron Emission. Since the previous work on diamond showed that its functionalization was closely connected with the ability to eject photoelectrons under illumination,[6] our first goal was to determine whether electron emission into the liquid was also of importance on amorphous carbon. Our measurements of work function and Fermi level position show that 4.9 eV incident photons (254 nm) have indeed sufficient energy to eject photoelectrons directly into a vacuum. Our photocurrent experiments also showed that substantial photocurrents, in the 0.2−1.5 nA range, are generated when the carbon/alkene interfaces are illuminated with 254 nm light. These experiments demonstrate that charged species are generated in the liquid phase upon illumination and strongly suggest that photoemission of electrons into the liquid phase plays a role in the grafting of amorphous carbon.

The photocurrents measured using TFAAD and tBOC are at least 2 orders of magnitude larger than those observed in control experiments with simple saturated alkanes such as dodecane (1−3 pA). These differences allow us to conclude that the significant photocurrent observed with TFAAD and tBOC arises from the photoinduced creation of charged species in the liquid phase and not from changes in photoconductivity of the carbon itself. Furthermore, they show that the photoconductivity is strongly dependent on the types of molecular groups present on the liquid-phase molecules. It is important to recognize that under steady-state conditions, the charge transfer of electrons and holes across the solid−liquid interface must balance. The overall situation is somewhat analogous (but complementary) to the use of TiO_2 as a photo-oxidizer. In the case of TiO_2, photoexcitation creates electron−hole pairs; the holes induce oxidation reactions of many organic species, but in order to maintain overall charge neutrality, a corresponding reduction reaction must take place. With TiO_2 this often occurs through a sacrificial molecule or contaminant, such as ambient water or oxygen.[62,63] While photoexcited TiO_2 is a strong oxidizer because its valence band is very low in energy, photoexcited diamond is effective at inducing reduction reactions because of the high energy of its conduction band, which lies even above the vacuum level (hence, its property of negative electron affinity). Amorphous carbon is an intermediate case. As in the previous work on diamond, there must be both oxidation and reduction reactions occurring simultaneously under steady-state conditions. However, it is possible for one of these reactions to control the photoconductivity and the rate of functionalization.

Our experimental data show that when comparing TFAAD and tBOC, there is a clear correlation in the extent of functionalization and in the observed photocurrents. TFAAD is the most reactive and yields the highest photocurrents, whereas tBOC yields much lower coverage and lower photocurrents. From this, we can conclude that the ability to functionalize is closely connected with the degree to which charged species are created in solution. Yet, this measurement alone does not establish whether the photoemission of electrons or the reactions of photoexcited hole states control the overall reactivity.

The critical role of photoelectron ejection is clearly identified by the density functional calculations showing that the four molecules have quite different electron affinities and, more importantly, that the trends in reactivity exactly parallel the differences in electron affinities: TFAAD has the lowest acceptor level (largest electron affinity) and yields the highest reactivity, tBOC and UA-Me are higher in energy (smaller EAs) and yield lower reactivity, and dodecene has the highest-lying acceptor level and yields the lowest reactivity. The donor levels, in contrast, are all very similar in energy. From this, we conclude that the photochemical reactivity correlates with the degree to which a given molecule is able to stabilize a negative charge.

(58) Robertson, J. *Mater. Sci. Eng., R* **2002**, *37*, 129−281.
(59) Pierson, H. O. *Handbook of Carbon, Graphite, Diamond and Fullerenes - Properties, Processing and Applications*; Noyes Publications: Park Ridge, NJ, 1993.
(60) Schmidt, W. F. In *Excess electrons in dielectric media*; Ferradini, C., Jay-Gerin, J.-P., Eds.; CRC Press, Inc.: Boca Raton, FL, 1991.
(61) Holroyd, R. A.; Russell, R. L. *J. Phys. Chem.* **1974**, *78*, 2128−2135.
(62) Lu, G.; Linsebigler, A.; Yates, J. T., Jr. *J. Phys. Chem.* **1995**, *99*, 7626−7631.
(63) Zhuang, J.; Rusu, C. N.; Yates, J. T., Jr. *J. Phys. Chem. B* **1999**, *103*, 6957−6967.

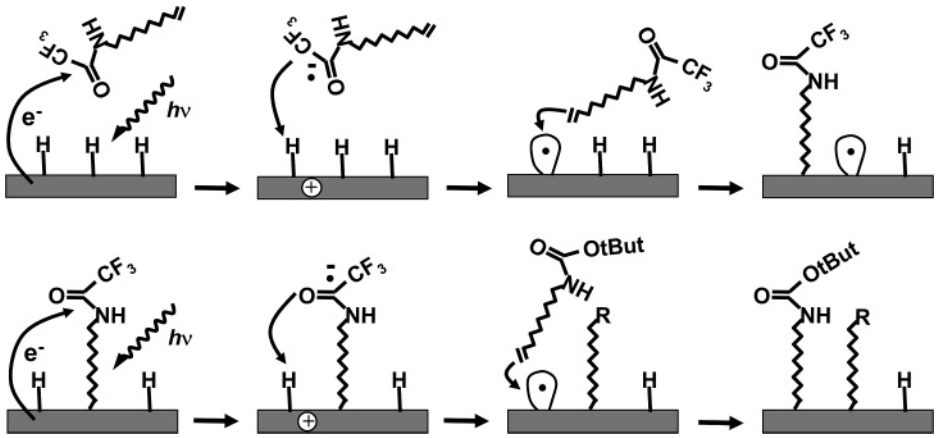

Figure 9. Proposed mechanism for the grafting of TFAAD on amorphous carbon and for the role of the TFAAD "seed" layer in the grafting of molecules with low reactivity such as tBOC.

While the electron affinities do not reflect the additional stabilization of ions in the condensed phase due to polarization of the surrounding dielectric, TFAAD and tBOC have similar structures and are therefore expected to have similar dielectric properties. These data strongly indicate that the photoelectron ejection controls the overall rate of reaction.

As shown in Figure 8, there are two distinct paths by which the electrons can be injected into the liquid. The first involves direct ejection from the carbon valence states into the alkene acceptor level via internal photoemission (Path 1). The second involves excitation of electrons to the conduction band via absorption of 4.9 eV photons by the carbon, followed by diffusion of the excited electrons toward the surface and into the acceptor level of the alkene (Path 2). In the case of diamond, both pathways have been proposed to explain sub-band gap electron emission into a vacuum, and it remains controversial which process dominates.[64−66] While our data on amorphous carbon do not allow us to definitively identify whether photoelectron emission arises from surface vs bulk excitations, we believe that direct surface excitation is likely dominant because the relatively high density of states starting ~0.5 eV below the Fermi energy and the work function 4.0 eV both facilitate the direct photoemission of electrons using 4.9 eV light. Additionally, carrier mobilities in amorphous carbon are quite low (~1×10^{-5} cm^2 V^{-1} s^{-1} for sputtered carbon)[67] thereby decreasing the likely importance of bulk electron−hole pairs.

For direct electron ejection into the liquid phase (internal photoemission), one would expect the efficiency of functionalization to correlate with the quantum yield of the internal photoemission process. The quantum yield for internal photoemission between two materials can be described according to Kane as[68]

$$R \approx (h\nu - \Phi)^p \qquad (3)$$

where $h\nu$ is the incident photon energy and Φ is the energy barrier to the process; the exponent p can have the values 1, $^3/_2$, 2, or $^5/_2$ depending on the type of emission mechanism. Based on our photoemission measurements and DFT calculations, the energy barriers for the different alkenes would be approximately 3.8 eV for TFAAD, 4.5 eV for UA-Me, 5.0 eV for tBOC, and 5.6 eV for dodecene, suggesting that dodecene and tBOC should be unreactive and UA-Me should be 3 to 12 times less reactive than TFAAD depending on the emission mechanism. These values appear to be in reasonably good agreement with our observations, again suggesting that the electron ejection process likely dominates the overall rate of reaction.

Photochemical Reaction and Charge Neutrality. While our data indicate that photoelectron ejection controls the overall photocurrent and the rate of functionalization, under steady-state conditions this electron ejection must be balanced by an equivalent oxidation reaction in order to maintain charge neutrality of the sample. Since the donor levels of the alkenes are very low in energy, it is unlikely that the alkenes themselves are reactive toward oxidation. Charge neutrality can then be maintained in two ways: (a) since electron emission forms anions immediately adjacent to the surface, the overall neutrality could be maintained by the abstraction of a proton by the anion or by its decomposition products; (b) a sacrificial molecule, such as residual water, could oxidize at the carbon surface. Since photoelectron ejection produces holes at the surface, the illuminated carbon surface is chemically similar to an alkyl radical cation, which in molecular systems is an excellent proton donor.[69−74] Proton abstraction from neutral species by radical anions has also been observed previously.[75−78] These prior results all indicate that either ionic or neutral reactive species in the liquid phase are likely to be suitable proton acceptors. Hypothesis (a) is depicted in Figure 9, in which the abstraction

(64) Bandis, C.; Pate, B. B. *Phys. Rev. Lett.* **1995**, *74*, 777−780.
(65) Nebel, C. E.; Shin, D.; Takeuchi, D.; Yamamoto, T.; Watanabe, H.; Nakamura, T. *Diamond Relat. Mater.* **2006**, *15*, 1107−1112.
(66) Takeuchi, D.; Ri, S. G.; Kato, H.; Nebel, C. E.; Yamasaki, S. *Phys. Status Solidi A* **2005**, *202*, 2098−2103.
(67) Evans, B. L.; Nasser, G. Y. *Phys. Status Solidi A* **1988**, *110*, 165−179.
(68) Kane, E. O. *Phys. Rev.* **1962**, *127*, 131−141.
(69) Demeyer, A.; Stienlet, D.; Ceulemans, J. *J. Phys. Chem.* **1994**, *98*, 5830−5843.
(70) Sviridenko, F. B.; Stass, D. V.; Molin, Y. N. *Mol. Phys.* **2003**, *101*, 1839−1850.
(71) Symons, M. C. R. *Pure Appl. Chem.* **1981**, *53*, 223−238.
(72) Mella, M.; Freccero, M.; Albini, A. *Tetrahedron* **1996**, *52*, 5533−5548.
(73) Mella, M.; Freccero, M.; Albini, A. *J. Chem. Soc., Chem. Commun.* **1995**, *1*, 41−42.
(74) Nicholas, A. M. D.; Arnold, D. R. *Can. J. Chem.* **1981**, *60*, 2165−2179.
(75) Born, M.; Ingemann, S.; Nibbering, N. M. M. *Mass Spectrom. Rev.* **1997**, *16*, 181−200.
(76) Hammad, L. A.; Wenthold, P. G. *J. Am. Chem. Soc.* **2000**, *122*, 11203−11211.
(77) McDonald, R. N.; Chowdhury, A. K.; McGhee, W. D. *J. Am. Chem. Soc.* **1984**, *106*, 4112−4116.
(78) Li, X.; Sanche, L.; Sevilla, M. D. *J. Phys. Chem. A* **2002**, *106*, 11248−11253.

of a proton by the initially formed radical anion leads to a neutral carbon "dangling bond". Subsequent steps in the reaction are then charge-neutral radical propagation steps. Previous studies of photochemical functionalization on silicon have shown that initiation of a silicon dangling bond can be followed by a propagation step involving abstraction of surface hydrogen by neutral radicals.[51,79] Due to the higher C−H bond strength it is not clear whether such a propagation step occurs on carbon substrates or whether the reaction terminates immediately.

It is important to consider that also processes that follow the reduction of alkenes in the liquid phase might be a factor in determining the reactivity. Dissociative attachment of the electron could generate radical fragments that display different reactivities in the case of our four alkenes. Such processes could indeed play a role since radical anions of trifluoroacetamides have been isolated and studied using electron spin resonance techniques and they have been shown to decay through the loss of radical and ionic fragments.[80−83] Also, electrochemical reductive dissociation reactions of alkyl and aryl halides have been extensively investigated, where the electron transfer results in the formation of a halide and a radical species of high reactivity that can lead to fast surface and/or volume reactions.[84−88] Hydrogen atom abstraction from the surface could take place as a result of a reaction between these decay products with the amorphous carbon;[89] therefore, the fate of trifluoroacetamide radical anions in the liquid phase might also be of significance for the reactivity of TFAAD.

Surface Seeding. The surface seeding experiments demonstrate that the presence of TFAAD enhances the reactivity of our carbon surfaces. To understand this, we note that the disappearance of the C═C and the vinyl C−H stretching bands in the IRRAS spectra of TFAAD upon grafting strongly suggests that the olefin moiety is lost during the grafting process and that it is directly involved in bonding to the surface. This conclusion is further supported by previous angle-resolved XPS measurements of TFAAD layers on diamond that showed that the trifluoroacetamide groups are located at the organic layer/vacuum interface,[6] and by chemical measurements showing that the TFAAD groups are chemically accessible.[8] Our results show that the presence of a relatively small number of TFAAD molecules on the surface greatly enhances the reactivity. We also observed that those absorption bands that are associated with the trifluoroacetamide group in the infrared spectra are lost upon grafting of the second alkene. The details of this effect are still under investigation. However, possible reasons for the spectral changes could be the loss of fluorine atoms from the protecting group, the deprotection of the entire trifluoroacetamide group, or a fragmentation of the initial layer along the hydrocarbon backbone.

These findings support the conclusions gathered from our theoretical studies of donor and acceptor levels. Figure 9 shows the proposed mechanism for the reaction via a "seed" layer. A first layer of TFAAD at low coverage is created through the grafting of TFAAD from solution onto a hydrogen terminated surface: the terminal trifluoroacetamide becomes the initiating radical anion species that abstracts a hydrogen, thus creating a first reactive site at the surface. The terminal groups now located at the surface serve as initiating species for the grafting of a second alkene through the same mechanism. The high coverage of the final layer compared to that of the initial TFAAD layer confirms that a radical mechanism is the basis of the grafting reaction.

5. Conclusions

Our results show that the photochemical functionalization of carbon surfaces with terminal alkenes proceeds through a complex mechanism. The use of amorphous carbon as a model material to understand the reaction mechanism is advantageous, given the ease with which organic layers can be characterized on its surface. Also, the electronic structure of our specific type of amorphous carbon can be pictured as intermediate between those of crystalline carbon materials at the two extremes of the carbon hybridization spectrum: diamond and graphite.

In the case of amorphous carbon, in agreement with previous findings on diamond,[6,11] the reaction is initiated by the absorption of a photon and the ejection of a photoelectron into the liquid phase. Photoejection emerges as a key step in the initiation of these reactions, and both the photoemission properties of the surface and the ability of the liquid to accept electrons are important for predicting the reaction efficiency. The overall reactivity trends observed in our work on amorphous carbon can therefore be significant in order to understand the reactivity of other semiconductors toward the photochemical functionalization of unsaturated organic compounds.

Our findings also provide a practical approach to overcome the intrisic reactivity limitations of specific molecules. Seeding substrates with surface-bound initiators could be a method of general applicability in order to expand the range of molecules that can be grafted using these reactions. Of all the molecules examined so far, TFAAD displays the highest reactivity, due to the presence of the highly electron-withdrawing trifluoroacetamide group that stabilizes photogenerated radical anions in the liquid phase. However, even better performance could potentially be achieved through careful tailoring of the electronic properties of the liquid phase: both the gas-phase electron-accepting properties of the alkene and the polarization properties of the liquid environment are factors that could be engineered in order to enhance the reactivity. It is interesting to point out that in the case of diamond a hydrogen-terminated surface was necessary to promote photoemission thanks to the negative electron affinity of hydrogen terminated surfaces.[6] However, in the case of amorphous carbon the requirement of hydrogen termination might be relaxed, as long as photoemission is still viable and other possible leaving groups are available at the surface in order to generate a reactive binding site. Indeed, the presence of surface bound species that can function as both electron acceptor and leaving group (e.g., chlorine atoms) might also constitute a surface termination that promotes reactivity.

(79) Eves, B. J.; Sun, Q. Y.; Lopinski, G. P.; Zuilhof, H. *J. Am. Chem. Soc.* **2004**, *126*, 14318−14319.
(80) Rogers, M. T.; Kispert, L. D. *J. Chem. Phys.* **1967**, *46*, 3193−3199.
(81) Chen, T. C. S.; Kispert, L. D. *J. Chem. Phys.* **1976**, *65*, 2763−2770.
(82) Samskog, P.-O.; Kispert, L. D. *J. Chem. Phys.* **1983**, *78*, 2129−2132.
(83) Toriyama, K.; Iwasaki, M. *J. Phys. Chem.* **1969**, *73*, 2663−2670.
(84) Andrieux, C. P.; Merz, A.; Savéant, J. M. *J. Am. Chem. Soc.* **1985**, *107*, 6097−6103.
(85) Andrieux, C. P.; Gallardo, I.; Savéant, J. M.; Su, K. B. *J. Am. Chem. Soc.* **1986**, *108*, 638−647.
(86) Andrieux, C. P.; Combellas, C.; Kanoufi, F.; Savéant, J. M.; Thièbault, A. *J. Am. Chem. Soc.* **1997**, *119*, 9527−9540.
(87) Savéant, J. M. In *Advances in Physical Organic Chemistry*; Tidwell, T. T., Ed.; Academic Press: San Diego, CA, 2000; Vol. 35.
(88) Hawley, M. D. In *Encyclopedia of electrochemistry of the elements*; Bard, A. J., Lund, H., Eds.; Marcel Dekker: New York, 1980; Vol. XIV.
(89) Togo, H. In *Advanced free radical reactions for organic synthesis*; Elsevier, Ltd.: Amsterdam, 2004.

There is great interest in developing chemistries that lead to semiconductor/organic interfaces with controlled functionalities in diverse areas such as sensing, energy storage, and conversion, as well as catalysis. These results could then provide guidelines for controlling the photochemical reactivity of organics on materials such as compound semiconductors and semiconducting and semimetallic nanostructures.

Acknowledgment. This manuscript is based on research supported by the National Science Foundation Grant CHE-0613010.

Supporting Information Available: Complete citation for ref 17; XPS and IRRAS data of control grafting experiments in the absence of UV illumination; reference FTIR spectra and spectral assignments of the alkenes used in this work; XPS and UPS spectra of "as deposited" carbon; impedance spectroscopy of H-terminated carbon; images of HOMO/SOMO surfaces and spin densities and optimized geometries (Zmatrix form) and energies of neutral and ionic species. This material is available free of charge via the Internet at http://pubs.acs.org.

JA073944Y